Journal of Electrotechnology, Electrical Engineering and Management (2023)
Clausius Scientific Press, Canada
DOI: 10.23977/jeeem.2023.060210
ISSN 2560-6697 Vol. 6 Num. 2

Research on power fluctuation matching control of large-scale wind power hydrogen production system based on multi-factor cyclic queue method

Hao Li[1,a], Zixuan Shangguan[1,b], Cunman Zhang[1,c,*]

[1]School of Automotive Studies, Tongji University, Shanghai, China
[a]2031660@tongji.edu.cn, [b]2010200@tongji.edu.cn, [c]zhangcunman@tongji.edu.cn
[*]Corresponding author

Keywords: Large-scale Wind Power Hydrogen Production, Alkaline Water Electrolyzer, Power Fluctuation Matching, Multi-factor Cyclic Queue

Abstract: Coupling and controlling renewable energy wind power and large-scale electrolytic hydrogen production system to adapt to the fluctuation of wind power can obtain green hydrogen energy from the source and reduce the waste phenomenon of renewable energy, so as to promote the development of a green and low-carbon energy society. In this paper, by constructing a large-scale electrolytic hydrogen production system with an alkaline water electrolyzer as the main body, a multi-factor cyclic queue control strategy developed based on the state parameters of the electrolyzer device is coupled, and the strategy simulation work is carried out in combination with the 241h wind power duration curve of a certain place. The simulation results show that the control strategy not only meets the requirements of the hydrogen production system for fast and accurate response to wind power fluctuation input, but also optimizes and balances the overall running time of the electrolytic hydrogen production system, effectively improving the life consistency of the hydrogen production system. The results of this study can provide a new technical development direction for large-scale consumption and application of renewable energy.

1. Introduction

At present, in order to cope with climate change and environmental pollution, all countries in the world are actively promoting the development of new energy application technologies for green and sustainable development, comprehensively reducing the consumption dependence of traditional fossil energy, so as to reduce the total carbon emissions at the national level as a whole until the goal of "peak carbon dioxide emissions" and "Carbon neutrality" is achieved. Research on the coupling conversion of Renewable Energy and hydrogen energy can solve the problem of wind power fluctuation stabilization for the future.

Alkaline water electrolysis (AWE) [1,2] is the electrolysis hydrogen production technology with the highest maturity in monetization operation, and it is also one of the popular choices for Renewable Energy hydrogen production technology selection. The dynamic response capability of the alkaline

water electrolyzer will affect the coupling control of renewable energy and the electrolyzer. Some researchers have studied the dynamic response characteristics of AWE through the coupling of AWE and the wind/photovoltaic fluctuating power supply [3-5], and the research has completed the research work on the dynamic response of the 250kW alkaline water electrolyzer [6]. These research results show that AWE has good dynamic response capability. Not only this, on the coupling control problem of hydrogen energy and renewable energy, researchers have also applied various control methods to the field of renewable energy hydrogen production [7-11]. For example, one study proposed a mixed integer linear programming model to solve the problem of low-cost hydrogen supply demand [12], and another study combined the advantages of simulated annealing algorithm and Genetic Algorithm to design and develop a renewable energy and hydrogen energy conversion control system [13].

These studies provide an important research basis for the research on power fluctuation adaptive control of renewable energy fluctuating power supply and large-scale electrolytic hydrogen production system. In this study, four different types of AWEs are used to build a large-scale electrolytic hydrogen production system, and based on the system state variables, the multi-factor cyclic queue method is used to adjust and control the fluctuating power of wind power, so as to realize the efficiency of the electrolytic hydrogen production system to the wind power. Efficiently follow the response target, and optimize the control of the system as a whole.

2. Alkaline Water Electrolyzer Model

In this study, the alkaline electrolytic cell in the electrolytic hydrogen production system will be modeled based on semi-empirical formulas. The model mainly refers to the relevant theoretical and empirical formulas for comprehensive consideration and establishment [14-18], which mainly includes the polarization curve part, the hydrogen production part and the thermal balance field part, and proposes improvements to the relevant parts based on the experience of test engineering measures. In the Table 1, it shows basic status information of four types of electrolyzers.

Table 1: Basic status parameters from four types of electrolyzers.

Type No.	Rated current (A)	Rated voltage (V)	Rated power (kW)	Number of cells	Rated hydrogen production rate ($Nm^3\ h^{-1}$)	A (m^2)
1	250	92	23	47	5	0.125
2	500	54	27	27	6	0.125
3	700	40	28	18	5	0.1167
4	1700	72	122.4	35	25	0.680

2.1 Polarization Curve

The basic form of the U - I polarization characteristics of electrolyzer for a given temperature used in this study can be expressed by

$$U = U_{rev} + (r_1 + r_2 \cdot T) \cdot \frac{I}{A} + (s_1 + s_2 \cdot T + s_3 \cdot T^2) \cdot \log\left(\left(t_1 + \frac{t_2}{T} + \frac{t_3}{T^2}\right) \cdot \frac{I}{A} + 1\right) \quad (1)$$

where U is the voltage of each cell, and U_{rev} is reversible cell voltage, and I is the current value of electrolyzer, and A is the area of electrode, which value is seen in the Table 1. And in the Eq. (1), the parameters of U – I polarization characteristics of electrolyzer are given in Table 2.

Table 2: Fitting parameters of polarization curve from four types of electrolyzers.

Type No.	1	2	3	4
$r_1(\Omega\ m^2)$	-1.295E-4	4.821E-5	-1.081E-5	5.761E-5
$r_2(\Omega\ m^2\ K^{-1})$	1.891E-6	-6.006E-7	3.503E-7	2.246E-7
$s_1(V)$	0.1962	0.114	0.3226	6.697E-2
$s_2(V\ K^{-1})$	5.761E-5	2.246E-7	6.697E-2	1.726E-3
$s_3(V\ K^{-2})$	1.614E-3	-5.158E-4	-3.788E-3	-1.746E-5
$t_1(A^{-1}\ m^2)$	2.696E-2	5.094E-2	1.199E-1	2.268E-1
$t_2(A^{-1}\ m^2K^{-1})$	-2.985	-9.332	-9.894	-25.53
$t_3(A^{-1}\ m^2K^{-2})$	146.9	464.4	251.2	877.4

2.2 Thermal Equilibrium Field

The temperature of electrolyzer is a basic variable that expresses the overall state of the electrolytic cell, and it affects the values of other state variables. Therefore, it is necessary to establish a heat balance field equation to characterize the temperature change of the electrolytic cell. Eq. (2) is the heat balance formula of the electrolytic cell.

$$C_t \cdot \frac{dT}{dt} = \dot{Q}_{gene} - \dot{Q}_{cool} - \dot{Q}_{loss} \tag{1}$$

n the Eq. (2), C_t represents the total heat capacity of electrolyzer (J K^{-1}), and other parameters can be calculated by the following Eq. (3) - (5)

$$\dot{Q}_{gene} = (U - U_{th}) \cdot N_{cell} \cdot I \tag{2}$$

$$\dot{Q}_{loss} = \frac{1}{R_t}(T - T_{am}) \tag{3}$$

$$\dot{Q}_{cool} = C_p\left(T_{out,cool} - T_{in,cool}\right) = LMTD \cdot (p_1 + p_2 \cdot I) \tag{4}$$

where U_{th} represents the thermal neutral voltage of electrolyzer, and N_{cell} is the number of cells of electrolyzer. In the Eq. (4), T represents the temperature of electrolyzer, and R_t represents the total heat resistance of electrolyzer (K W^{-1}), T_{am} represents the ambient temperature. In the Eq. (5), C_p represents the cooling water heat capacity (J K^{-1}) which is calculated by Eq. (6), $T_{out,cool}$ and $T_{in,cool}$ represents the inlet and outlet temperature of cooling water (K), and $LTMD$ represents the logarithmic average temperature difference between the electrolyzer and the heat exchanger, which is calculated by Eq. (7), p_1 and p_2 is the heat exchange coefficient.

$$C_p = \frac{\rho_{H_2O} \cdot V_{cool} \cdot Cp_{H_2O}}{M_{H_2O}} \frac{1000}{3600} \tag{5}$$

$$LMTD = \frac{(T - T_{in,cool}) - (T - T_{out,cool})}{\ln(T - T_{in,cool}) - \ln(T - T_{out,cool})} \tag{6}$$

$$T_{out,cool} = T_{in,cool} + \left(T - T_{in,cool}\right) \cdot \left(1 - \exp\left(-\frac{(p_1 + p_2 \cdot I)}{C_p}\right)\right) \tag{7}$$

In the Eq. (6), ρ_{H_2O} is the density of water, and V_{cool} represents the flow of cooling water, and Cp_{H_2O} is the thermal capacity of water, and M_{H_2O} is the molar mass of water. Those parameters above are regarded as constants.

Therefore, after solving the cooling water outlet temperature according to Eq. (8), we can substitute Eq. (3)-(8) into Eq. (2) to obtain the temperature change value of the thermal equilibrium field. Other relevant parameters in the calculation process are shown in the table 3.

Table 3: Fitting parameters of thermal equilibrium field from four types of electrolyzers.

Type No.	C_t ($J\ K^{-1}$)	R_t ($K\ W^{-1}$)	p_1 ($W\ K^{-1}$)	p_2 ($W\ K^{-1}\ A^{-1}$)
1	6.362E5	0.0971	7.975	0.7206
2	5.4897E5	0.1854	8.212	0.4375
3	4.4307E5	0.0694	18.97	0.2498
4	2.0911E6	0.0104	12.19	0.5789

2.3 Hydrogen Production

The hydrogen production rate for several cells connected in series is expressed by

$$\dot{n}_{H_2} = \frac{22.4\eta \cdot N_{cell} I}{3.6zF} \tag{8}$$

where $\dot{n}_{H_2}$ is the hydrogen production rate of electrolyzer ($Nm^3\ h^{-1}$), and η represents the faraday efficiency of electrolyzer. z is the electron transfer number of each reaction, which value is 2, and F represents the faraday constant, which value is 96485 C mol^{-1}.

$$\eta = a_1 + a_2 \cdot \exp\left(\frac{a_3 + a_4 \cdot T + a_5 \cdot T^2}{\frac{I}{A}}\right) \tag{9}$$

The faraday efficience fitting parameters of electrolyzer are given in Table 4.

Table 4: Fitting parameters of faraday efficience from four types of electrolyzers.

Type No.	a_1 -	a_2 -	a_3 ($A\ m^{-2}$)	a_4 ($A\ m^{-2}\ K^{-1}$)	a_5 ($A\ m^{-2}\ K^{-2}$)
1	0.9901	-8.14E-7	200.2	-5.515	0.7626
2	0.99	-5.14E-6	-235.3	-8.812	-0.763
3	0.9496	-5.27E-6	2.214	10.7193	-0.02509
4	0.9821	-0.02891	215.5	-3.473	0.02816

3. Multi-factor Cyclic Queue Control Strategy

3.1 Definition of Concept

- *Node*: It represents the electrolyzer unit in electrolytic hydrogen production system.
- *Solution space*: It represents the solution space range of all nodes in the electrolytic hydrogen production system.
- *Solution set*: For the current input power, the control algorithm picks the combination of nodes from the solution space for power matching.
- *Maximum capacity load power* (*MCLP*): For different temperature states of the node, under the safety setting that satisfies the cell protection voltage of the node (set to 2.1V in this study), the maximum safe load power that the node can allow.
- *Running time* (RT): It refers to the total startup time of the node that it is put into operation, and it is not counted when the node is in a shutdown or fault state.
- *Sorting factor* (SF): It refers to those variables which can be calculated according to the state parameters of the node. Generally, some state parameters of the node could be directly taken as the sorting factor.

3.2 Description of Strategy

Figure 1 describes the control logic of a multi-factor cyclic queue. Generally, the faulty node in the system does not participate in any process of the cyclic queue. The specific process is that the strategy performs multi-factor sorting according to the previous state sequence. Firstly, the sorting method is to compare the factor values of the nodes factor by factor from high to low according to the priority level of the factors, until the order of the comparing nodes can be judged, just like in Fig. 1, the factor 1 with the highest priority level of $node_K$ and $node_{K+1}$ can already judge the mutual order of the nodes, so the later factors do not need to be compared. In a sum, the node sorting criterion is to follow the factor values are arranged in descending order, so that the queue has completed the update operation.

After that, the algorithm needs to check the total RT of the running nodes in the previous state, selects the nodes that exceed the upper limit of the set average RT to join the tail of the queue according to the dequeuing order and makes other nodes in the queue to update their queue positions in turn. Therefore, the overall algorithm flow is like forming a circular queue that alternately operating and updates. Using this strategy can not only achieve the optimal matching goal of the optimal node, but also avoid the problem of excessive extreme difference in the RT between the nodes of the hydrogen production system, even affecting the overall life consistency of the system.

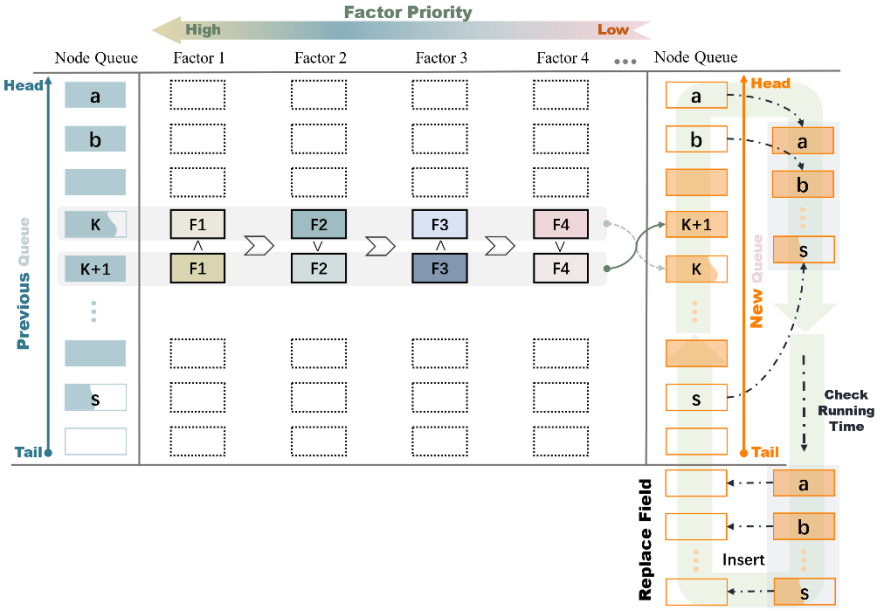

Figure 1: Diagram of the principle of multi-factor cyclic queue.

3.3 Distribution Method of Wind Power Based on Multi-factor Cyclic Queue Strategy

After the update of the cyclic queue is completed, the power matching can be performed according to the input wind power. After completing the multi-factor sorting of the previous queue based on the picked SFs and the RT inspection process, the previous queue is transformed to a new cyclic queue, and the node order of the queue is the power distribution order. The solution set of power distribution is the sub-sequence from the head node to the last node that can be assigned to power in the new cyclic queue, and the allocated power of each node in solution set is basically its own MCLP value.

In addition, the power distribution value of each node needs to be based on the node's MCLP rather than the node's rated power to complete the matching adaptation of the hydrogen production system to the input wind power. However, at the end of the power distribution, there may be a situation where

the power distribution cannot meet the MCLP of the last node, so the load current value corresponding to the allocated power of the node needs to be calculated.

MCLP is calculated as the follow steps:

Step 1: Get node temperature T, maximum loading current I, protection voltage U_{safe}.

Step 2: Calculate cell voltage V at current I and temperature T by using polarization curve model.

Step 3: Determining whether V is greater than U_{safe}, and if so, the loading current value I is decreased by 1% and return to Step 2, otherwise, the process proceeds to the next step.

Step 4: Calculate the product of the cell voltage V and the loading current value I, that is MCLP.

Step 5: Output load current value I and MCLP.

4. Simulation of System

4.1 Data Basis of Simulation

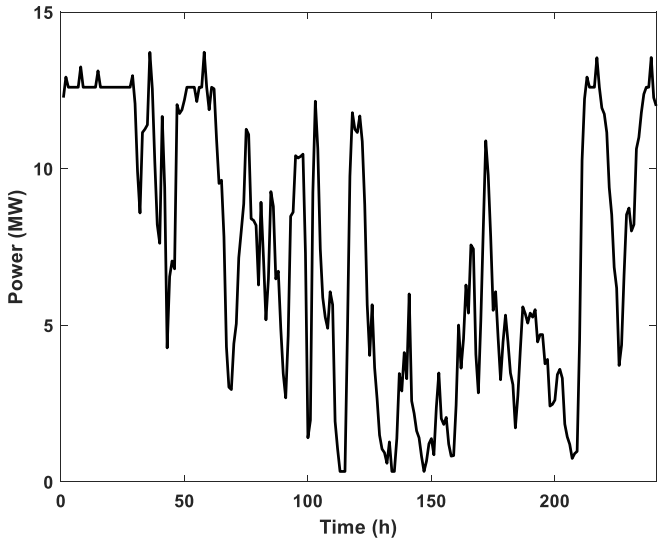

Figure 2: Wind power curve of simulation input.

In this study, the wind power sampling data of 241h in a certain area will be used to carry out the system simulation work, and the wind power curve is shown in Figure 2. Since the length of the wind power sampling time is one hour, which is not conducive to the state simulation of the electrolytic hydrogen production system, the node simulation time step for the electrolytic hydrogen production system is set to 120 seconds. The number of each type of electrolyzer in the simulated electrolytic hydrogen production system is shown in Table 5.

Table 5: Number of each type of electrolyzer in electrolytic hydrogen production system.

Type No.	1	2	3	4
Number	35	41	43	185

In the multi-factor selection, the main goal of the system simulation is to achieve dynamic follow-up of wind power, optimal matching, and ensuring system life consistency. Therefore, this study selects four state parameters of electrolyzer as SFs of Multi-factor Cyclic Queue Strategy, which are the operating temperature T, the maximum capacity load power MCLP, the hydrogen production faraday efficiency η and the running time RT. And the priority of SFs from high to low is T, MCLP, η and RT, as shown in Table 6.

Table 6: Selected multi-factor corresponding variables.

Sorting Factor	1st Factor	2nd Factor	3rd Factor	4th Factor
Variable Name	t	MCLP	η	rt

In addition, the ambient temperature of each electrolyzer of the electrolytic hydrogen production system is set a rand number between 5 K and 25 K, and the threshold value of RT of the hydrogen production system is set to 24 h in the control strategy. The cooling water flow of each type of electrolyzer is shown in Table 7.

Table 7: Cooling water flow of each type of electrolyzer.

Type No.	1	2	3	4
Cool Water Flow (m^3/h)	0.4	0.46	0.37	1

4.2 Flowchart of the Simulation System

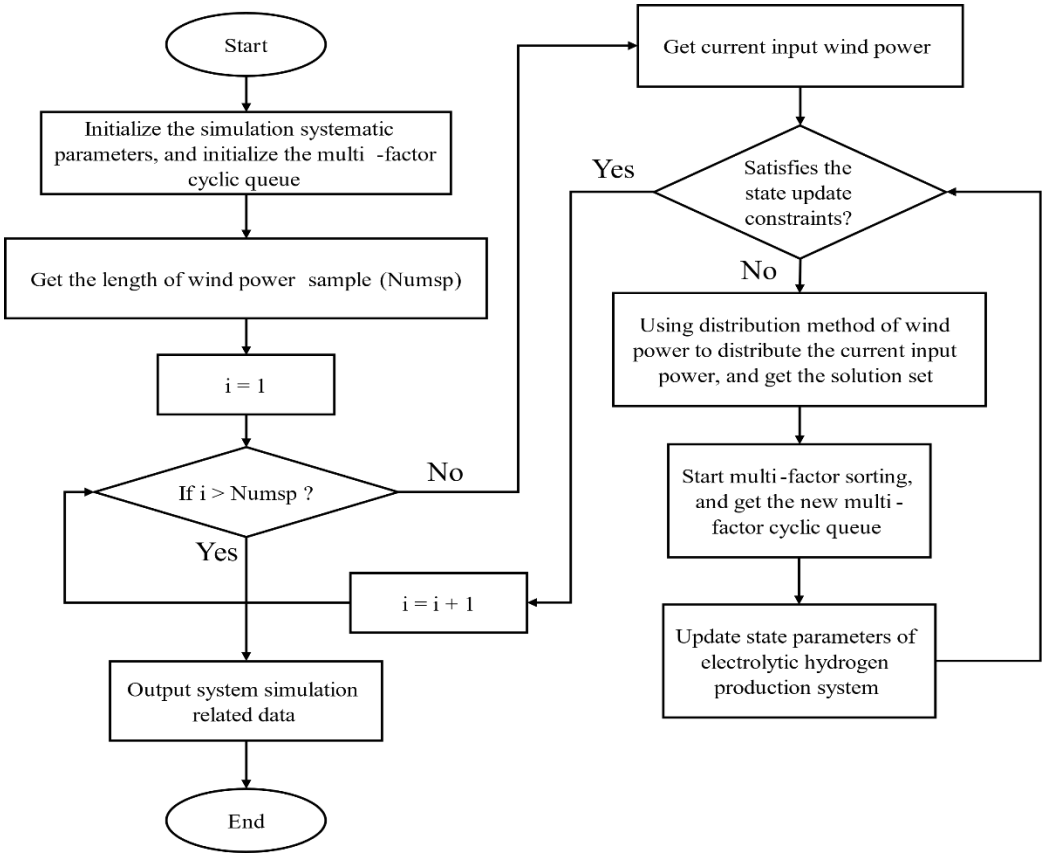

Figure 3: Flowchart of the system simulation algorithm.

The simulation flowchart of system is shown in Fig. 3. The relevant components of the simulation system are constructed by MATLAB, and the relevant simulation data will be saved during the simulation calculation process, which is finally exported uniformly at the end of the simulation.

5. Results and Discussion

5.1 Analysis of Overall Simulation

Figure 4 shows the power following situation and the matching error statistics. As can be seen from the figure a in Fig. 4, the system load power can quickly adapt to the fluctuation of the wind

power input power, and the RMSE between the following response power and the wind power input power which is obtained by Eq. (11) is about 0.06. These outcomes indicate that under the multi-factor cyclic queue control strategy, the electrolytic hydrogen production system has good following performance for the fluctuating wind power. As can be seen from the figure b, most of simulation point's error values between the power matching of the simulation system and the input wind power are concentrated within 10%, and the high proportion error is mainly in the low power stage. In addition, most of the error values are in the upper triangle area, indicating that the sum of the load power of the matched nodes of the system is greater than the input wind power, which meets the basic control requirements of power fluctuation adaptive control.

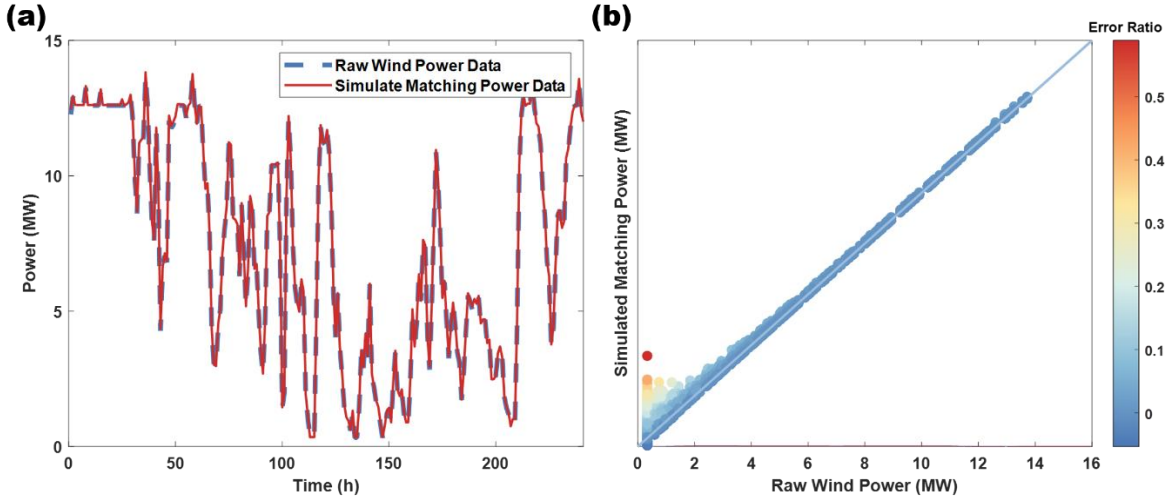

Figure 4: (a) The following response of the simulated matched power and the original wind power is shown; (b) is the error statistics of matching power and original wind power.

The root mean square error (RMSE) is usually used to evaluate the accuracy between the estimated results and the experimental data. The formula is as follows:

$$\mathrm{RMSE} = \sqrt{\frac{1}{n}\sum_{i=1}^{n}(\hat{x}_i - x_i)^2} \tag{10}$$

where $\hat{x}_i$ represents the estimated value of the estimation method, x_i represents the real value in the test data result, and n is the number of estimated values.

5.2 Matching Analysis within a Single Power Sampling Time

In conjunction with Fig. 5 and Fig. 6, it can be analyzed that there are also differences in the matching follow-up of wind power by the system at different power sampling times. The 120th hour's wind power follow-up response error shown in Fig. 5 is less than the 121th hour's error shown in Fig. 6 at the next time, and its fluctuation amplitude of wind power follow-up response should also be smaller. However, the overall fluctuation follow-up error extreme value is limited within 0.05 MW, which is within a controllable range for the cluster system.

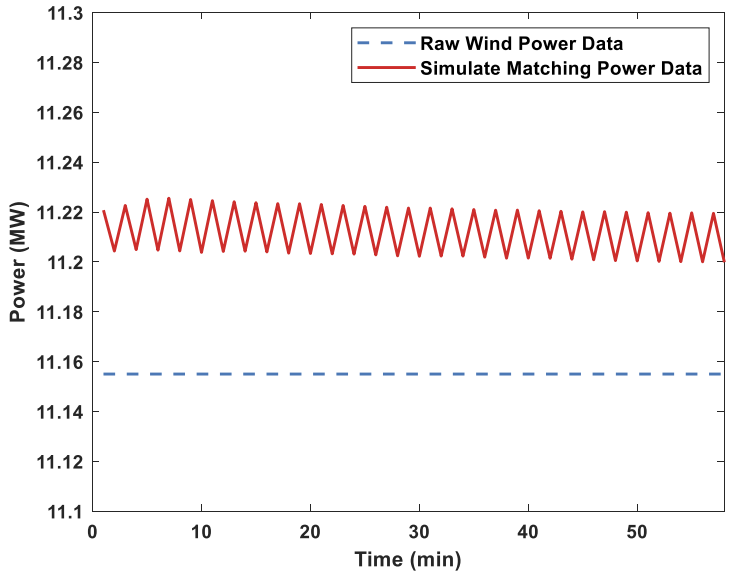

Figure 5: Power response following within the 120th hour power sample time.

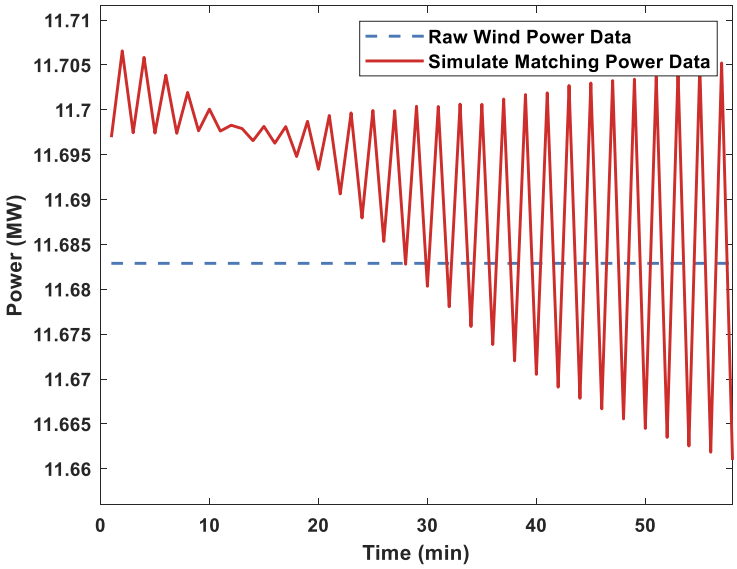

Figure 6: Power response following within the 121th hour power sample time.

5.3 Analysis of Classic Conditions

5.3.1 Analysis of Power Surge Condition

The power plunge condition is selected from the sampling points with the maximum increase according to the simulated power curve (the wind power increases 7.273 MW, and the ratio is 517.4%). The number distribution and power distribution of four types of electrolyzers are shown in Table 8 and Table 9. It can be seen that the changes in the solution set before and after the power surge condition are the same in the number of the 2^{nd}, 3^{rd} and 4^{th} types of electrolyzers, all of which are 3. And the matching power increase is also based on the average MCLP of each type of electrolyzer to change.

Table 8: The matching number of electrolyzer types under the power surge condition.

Type No.	1	2	3	4
Previous Status Number	0	1	1	12
Current Status Number	0	4	4	15

Table 9: The matching power of electrolyzer types under the power surge condition.

Type No.	1	2	3	4
Previous Status Power(kW)	0	28.1	25.9	1351.6
Current Status Power(kW)	0	112.7	103.4	1752.3

5.3.2 Analysis of Power Plunge Condition

The power plunge condition is selected from the sampling points with the maximum drop according to the simulated power curve (the power drop level is 5.902 MW, and its ratio is 56.4%). The number distribution and power distribution of four types of electrolytic cells are shown in Table 10 and Table 11. As can be analyzed, the change of the solution set before and after the power under such power plunge condition is quite different. And the optimization strategy will perform head optimization according to the current cyclic queue state, because under the control of multi-factor sorting strategy, the number of four types of electrolyzers is different, resulting in different decreasing proportions of matching solution sets.

Table 10: The matching number of electrolyzer types under the wind power plunge condition.

Type No.	1	2	3	4
Previous Status Number	13	20	14	81
Current Status Number	10	12	13	56

Table 11: The matching power of electrolyzer types under the wind power plunge condition.

Type No.	1	2	3	4
Previous Status Power(kW)	298.2	563.3	216.3	9384.9
Current Status Power(kW)	237.2	337.6	287.0	6445.3

5.4 Analysis of Runtime Consistency

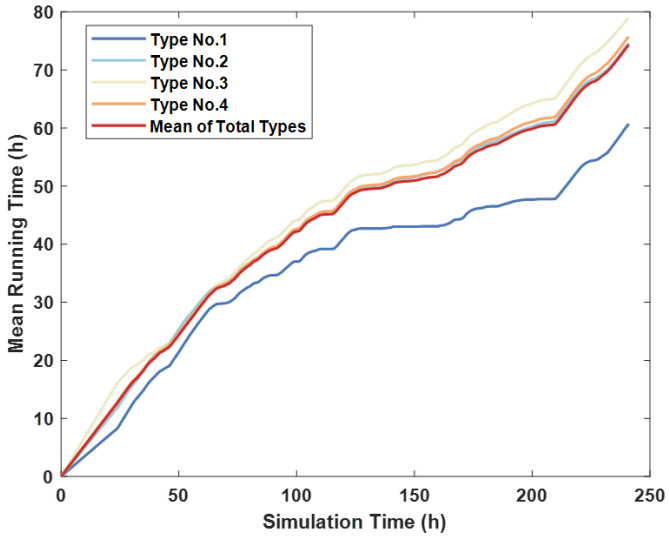

Figure 7: The mean running time curves of different types of electrolytic cells.

As can be seen from Figure 7, the variation trend of the mean running time of all types of electrolyzers is roughly the same, which indicates that the multi-factor Cyclic Queue Control Strategy has strong randomness when selecting different types of electrolyzers nodes and putting them into operation, and can ensure the mean life of various types of electrolyzers to reach good consistency. At the same time, we can also analyze that the curves of Type No.2 and Type No.4 are close to the overall average running time curve of the system, that in different power load conditions, the number of these two types of electrolyzers that can be used is relatively more frequent firstly. Secondly, because there are differences in the temperature loading characteristics of different types of electrolyzers, and the operating temperature in the selection sorting factor is the highest priority, which will reduce the possibility that the nodes with poor loading characteristics are preferentially selected into power matching process.

6. Conclusion

In this paper, a dynamic simulation model for alkaline water electrolyzer is introduced, and a control strategy based on the idea of multi-factor sorting that can be applied to large-scale wind power hydrogen production systems for power fluctuation adaptation is proposed. A multi-factor cyclic queue that can update the power fluctuation matching solution set of the electrolytic hydrogen production system in real time. The case simulation results show that the proposed multi-factor cyclic queue control strategy can quickly respond to various conditions of the wind power fluctuations, and its simulation following accuracy is above 95%. In addition, the optimal control strategy by setting the running time can effectively ensure a good life consistency of the electrolytic hydrogen production system. Since the control strategy is controlled based on the state of the electrolytic hydrogen production system, it can be extended to the research on the power fluctuation adaptation control of the GW-level wind power scale and the MW-level electrolytic hydrogen production system, which is useful for the further coupling application to large-scale renewable energy and hydrogen and provides a good research foundation.

References

[1] Amores E, Rodr ́guez J, Carreras C. Influence of operation parameters in the modeling of alkaline water electrolyzers for hydrogen production [J]. International Journal of Hydrogen Energy, 2014, 39(25): 13063-78.

[2] Santos DMF, Sequeira CAC, Figueiredo JL. Hydrogen Production by Alkaline Water Electrolysis [J]. Quimica Nova, 2013, 36(8): 1176-93.

[3] Hug W, Bussmann H, Brinner A. Intermittent operation and operation modeling of an alkaline electrolyzer [J]. International journal of hydrogen energy, 1993, 18(12): 973-7.

[4] Hug W, Divisek J, Mergel J, et al. Highly efficient advanced alkaline electrolyzer for solar operation [J]. International Journal of Hydrogen Energy, 1992, 17(9): 699-705.

[5] Urs úa A, Sanchis P. Static–dynamic modelling of the electrical behaviour of a commercial advanced alkaline water electrolyser [J]. International Journal of Hydrogen Energy, 2012, 37(24): 18598-614.

[6] Zhang C, Wang J, Ren Z, et al. Wind-powered 250 kW electrolyzer for dynamic hydrogen production: A pilot study [J]. International Journal of Hydrogen Energy, 2021, 46(70): 34550-64.

[7] Fang Ruiming, Liang Yin. Control strategy of electrolyzer in a wind-hydrogen system considering the constraints of switching times [J]. International Journal of Hydrogen Energy, 2019, 44(46): 2510425111.

[8] Cai Guowei, Peng Long, Kong Lingguo, et al. Power coordinated control of solar-hydrogen hybrid power generation system [J]. Automation of Electric Power Systems, 2017, 41(1): 109-116.

[9] Deng Hao, Chen Jie, Jiao Dongdong, et al. Energy management control strategy of wind hydrogen coupling combined power grid system [J]. High Voltage Technology, 2020, 46(1): 99-106.

[10] Flamm B, Peter C, Büchi FN, et al. Electrolyzer modeling and real-time control for optimized production of hydrogen gas [J]. Applied Energy, 2021, 281

[11] Liu Z, Zhang Z, Zhuo R, et al. Optimal operation of independent regional power grid with multiple wind-solar-hydro-battery power [J]. Applied Energy, 2019, 235(1541-50).

[12] Khalilnejad A, Riahy G H. A hybrid wind-PV system performance investigation for the purpose of maximum

hydrogen production and storage using advanced alkaline electrolyzer [J]. Energy Conversion & Management, 2014, 80(apr.): 398-406.
[13] Carapellucci R, Giordano L. Modeling and optimization of an energy generation island based on renewable technologies and hydrogen storage systems [J]. International Journal of Hydrogen Energy, 2012, 37(3):2081-2093.
[14] Ystein U. Modeling of advanced alkaline electrolyzers: a system simulation approach [J]. International Journal of Hydrogen Energy, 2003,
[15] Ursúa A, Sanchis P. Static–dynamic modelling of the electrical behaviour of a commercial advanced alkaline water electrolyser [J]. International journal of hydrogen energy, 2012, 37(24): 18598-614.
[16] Haug P, Kreitz B, Koj M, et al. Process modelling of an alkaline water electrolyzer [J]. International Journal of Hydrogen Energy, 2017, 42(24): 15689-707.
[17] Sánchez M, Amores E, Rodríguez L, et al. Semi-empirical model and experimental validation for the performance evaluation of a 15 kW alkaline water electrolyzer [J]. International Journal of Hydrogen Energy, 2018, 43(45): 20332-45.
[18] Milewski J, Guandalini G, Campanari S. Modeling an alkaline electrolysis cell through reduced-order and loss-estimate approaches [J]. Journal of Power Sources, 2014, 269, 203-11.